SCIENTIFIC REPORTS

OPEN

SUBJECT AREAS:
ANIMAL BEHAVIOUR
NEUROSCIENCE

Received
18 November 2013

Accepted
31 December 2013

Published
22 January 2014

Correspondence and requests for materials should be addressed to D.-Y.C. (chendy@nankai.edu.cn); X.Z. (zhaoxin@nankai.edu.cn) or X.-Z.F. (xzfeng@nankai.edu.cn)

* These authors contributed equally to this work.

SiO_2 nanoparticles change colour preference and cause Parkinson's-like behaviour in zebrafish

Xiang Li[1]*, Bo Liu[2]*, Xin-Le Li[3]*, Yi-Xiang Li[1], Ming-Zhu Sun[2], Dong-Yan Chen[3], Xin Zhao[2] & Xi-Zeng Feng[1]

[1]State Key Laboratory of Medicinal Chemical Biology, College of Life Science, Nankai University, Tianjin 300071, China, [2]The Institute of Robotics and Automatic Information Systems, Nankai University, Tianjin 300071, China, [3]The Key Laboratory of Animal Models and Degenerative Diseases, Department of Physiology, School of Medicine, Nankai University, Tianjin, 300071, China.

With advances in the development of various disciplines, there is a need to decipher bio-behavioural mechanisms via interdisciplinary means. Here, we present an interdisciplinary study of the role of silica nanoparticles (SiO_2-NPs) in disturbing the neural behaviours of zebrafish and a possible physiological mechanism for this phenomenon. We used adult zebrafish as an animal model to evaluate the roles of size (15-nm and 50-nm) and concentration (300 μg/mL and 1000 μg/mL) in SiO_2-NP neurotoxicity via behavioural and physiological analyses. With the aid of video tracking and data mining, we detected changes in behavioural phenotypes. We found that compared with 50-nm nanosilica, 15-nm SiO_2-NPs produced greater significant changes in advanced cognitive neurobehavioural patterns (colour preference) and caused potentially Parkinson's disease-like behaviour. Analyses at the tissue, cell and molecular levels corroborated the behavioural results, demonstrating that nanosilica acted on the retina and dopaminergic (DA) neurons to change colour preference and to cause potentially Parkinson's disease-like behaviour.

Because of their unique physicochemical properties (i.e., small particle size, large surface area and high drug-loading efficiency), SiO_2-NPs have been widely employed[1] in fields such as plastic manufacturing and agriculture and in products such as bactericidal agents and paint. SiO_2-NPs have also been developed for biomedical purposes, such as bioimaging[2], cancer treatment[3], targeted and controlled drug delivery and release[4] and gene transduction[5]. Thus, with the increasingly extensive employment of SiO_2-NPs, there is great concern regarding the potential effects of SiO_2-NPs on terrestrial and aquatic organisms, especially on humans[6]. Fortunately, substantial work concerning the toxicological impacts of SiO_2-NPs has been published. Boxall, BA. A. *et al.* studied the size distribution of SiO_2-NPs (from 135 nm to 510 nm) dispersed in water and their potential risks to aquatic living organisms[7]. Furthermore, depending on their size and chemical composition, nanoparticles may bypass the blood-brain barrier (BBB) and gain direct entry into the brain[8,9]. Wu, J. *et al.* used Sprague Dawley rats (SD rats) as an animal model and determined that SiO_2-NPs delivered via intranasal instillation passed through the BBB, entered the brain and may have exerted a negative impact on the striatum and DA neurons, as well as increasing the potential risk of neurodegenerative diseases[10]. Schafer, D. P. *at el.* demonstrated that very low levels of SiO_2-NPs were capable of altering microglia, whose functions may protect the body from degenerative brain disease[11]. Increased ROS and RNS production, as well as changes in proinflammatory genes and cytokine release, may adversely affect not only microglial function but also surrounding neurons. Furthermore, Deleidi, M. *et al.* suggested that inflammation may trigger neurodegenerative diseases[12]. Overall, the results of these studies suggest that there is an underlying neurotoxicity of SiO_2-NPs and a potential hazard for neurodegenerative dysfunction.

Due to its genetic homology with most human genes, including neurodegenerative genes[13–22], the zebrafish has recently been applied as a model for many neurodegenerative diseases, including Parkinson's disease[23] and Huntington's disease[24–26]. With the establishment of increasing numbers of transgenic or drug-induced neurodegenerative models, there is a need to evaluate the advanced neurobehavioural (learning and memory) and locomotive activities (decreased locomotive activity underlying Parkinson's-like behaviour) in these models. Most learning and memory assays are based on colour discrimination and are correlated with a visual stimulus[27]. Relatively few studies have evaluated the impacts of the unique properties of NPs, such as particle size, on neurobehavioural function. Although our previous work assessed the effects of silica size on the rest/wake behaviour of zebrafish larvae[28], there is a paucity of research examining the size and concentration effects of

NPs, especially SiO_2-NPs, on the advanced cognitive behaviour of adult zebrafish. Specifically, there is a lack of data on colour preference, which is essential for learning and memory in mature fish. Furthermore, relatively few researchers have focused on the neurodegenerative disease-like behaviours induced by SiO_2-NPs in zebrafish via comprehensively and meticulously analysing numerical and spatial changes in locomotive activities.

In this study, we simulated the pollution of an aquatic system with engineered SiO_2-NPs with the aim of discovering the influence of SiO_2-NPs of different sizes and concentrations on the neurobehaviours of aquatic vertebrates such as zebrafish. The innovative goal of our research was to employ neurobehavioural science to discover whether the presence of nanosilica in an aquatic environment poses a risk to an aquatic organism (zebrafish) by measuring the cognitive behaviours and locomotive activities of the organism. We analysed the effects of nanosilica size and concentration on zebrafish behaviour; specifically, we examined the differences between the effects of 15-nm and 50-nm SiO_2-NPs on the neurobehaviours of zebrafish. In light of the potential hazards of silica nanoparticles to the central nervous system (CNS), we found that nanosized silica could induce neurodegenerative disease-like behaviours in adult zebrafish and hence have introduced a neurodegenerative disease behavioural model in zebrafish.

Results

Behaviour recordings and nanoparticle and colour characterisations. Zebrafish treated with silica nanoparticles of different sizes and concentrations were transferred to a colour combination-enhanced CPP apparatus for behavioural recording (Fig. 1A). We analysed locomotive activity and colour preference parameters using self-designed zebrafish behavioural analysis software (Supplementary Figures S1–2). We present the real-time velocity parameter test results of selected zebrafish (Fig. 1D). There was a trend for the locomotive values of the nanosilica-treated zebrafish to be lower than those of the wild-type zebrafish and for the nanosilica to disturb the colour preference of the zebrafish (Supplementary Figure S3). In the nanosilica-treated groups, the locomotive values of the 15-nm groups were lower than those of the 50-nm groups at same concentration.

The four colour papers used in this experiment were characterised with Shimadzu UV-3600 UV-VIS-NIR photospectrometer (Shimadzu Co., Japan). The reflectance spectra of the four different coloured papers are shown in Fig. 1C. The peak wavelengths of the coloured papers were 449.45 nm (blue), 535.37 nm (green), 577.33 nm (yellow) and 659.75 nm (red); these wavelengths are comparable to colour vision with peaks of ultraviolet (362 nm), violet (415-nm), cyan (480 nm) and yellow (570 nm) in zebrafish[28–30]. DLS was used to determine the size and charge of SiO_2-NPs dissolved in standard tank water. The agglomeration size increased when the concentration was higher and the size of the silica was larger. The mean particle sizes and zeta potentials of the SiO_2-NPs of different sizes and concentrations in standard tank water are presented in Supplementary Table S1.

Impact of SiO_2-NPs on colour preference behaviour and locomotive activities. To assess the impacts of SiO_2-NP size and concentration on the cognitive and motor behaviours of zebrafish, hierarchical clustering was employed as an unsupervised statistical and semiquantitative method to generally classify nine behavioural parameters according to the effects of SiO_2-NPs of different concentrations and sizes (Fig. 2A). The degree of similarity of the data between the four experimental groups suggests that the SiO_2-NPs of different sizes and concentrations produced similar degrees of changes in behavioural parameters. For the experimental treatment, the hierarchical clustering analyses showed that the data from the 15-nm 1000 μg/mL group and the 50-nm 300 μg/mL group could first be clustered according to the degree of similarity between the influence of the different groups on all the behaviours. The data from Cluster I (15-nm 1000 μg/mL and 50-nm 300 μg/mL) and from the 50-nm 1000 μg/mL group were then combined into Cluster II. Finally, due to the unique properties of the data from the 15-nm 300 μg/mL group, this group was categorised as a single cluster, Cluster III. For the behavioural parameter clustering, SiO_2-NP treatment broadly changed the behavioural patterns of adult zebrafish, with the majority of the behavioural data deviated from the norm.

To identify the specific effects of SiO_2-NPs of different sizes and concentrations on behavioural parameters in six colour combinations, we performed statistical analyses of nine behavioural parameters (Fig. 2B). For the parameter "stay time", in all six colour combinations, there was a trend that the SiO_2-NP-treated zebrafish spent more time in the red compartment and less time in the green, yellow and blue compartments compared with the wild-type zebrafish (control group). At the same concentration, the 15-nm treated group exhibited more significant differences than the 50-nm treated group. At the same nanosize, a high concentration (1000 μg/mL) had a stronger effect than a low concentration (300 μg/mL). For all the SiO_2-NP-treated groups, the column chart showed that SiO_2-NP treatment changed the colour preference of zebrafish within the group (Supplementary Figure S5 A–C).

For the parameter "distance", SiO_2-NP treatment decreased the total swimming distance of zebrafish during the 180-s test. Of all the experimental treatments, 15-nm 1000 μg/mL exerted the greatest impact on swimming distance. However, the swimming distance in the red colour compartment was relatively increased. For the parameter "thigmotaxis", SiO_2-NP treatment enhanced the thigmotaxis towards the red colour compartment. There was a trend that SiO_2-NP treatment decreased the locomotive activity (the distance, velocity, turn angle and angle velocity parameters); the 15-nm SiO_2-NP group had significantly lower values compared with the 50-nm group. The specific locomotive patterns (freezing, swimming and rapid motive time ratio) were also disturbed, particularly by the 15-nm SiO_2-NPs. SiO_2-NP treatment not only changed the natural mode of the locomotive activities of the zebrafish in the different groups, it also disturbed the normal pattern of the locomotive activities of the wild-type zebrafish in all the groups (Supplementary Figure S5 D–I).

Impact of SiO_2-NPs on the swimming path of zebrafish. We further investigated the effects of SiO_2-NPs of different sizes and concentrations on the spatiotemporal swimming patterns of zebrafish (Fig. 3A). The trajectories of wild-type zebrafish are intensive, and the scope of their swimming area is wide. The wild-type zebrafish exhibited a normal colour preference order, demonstrating a greater preference for blue and green than for red and yellow. However, SiO_2-NP treatment decreased the zebrafish locomotive activities and disturbed their swimming path patterns and colour preference. In general, SiO_2-NPs decreased all the locomotive activities in six colour combinations, resulting in sparse trajectories and reduced swimming activity. The pattern of the swimming path also changed. Furthermore, SiO_2-NP treatment increased the preference for red and decreased the preference for blue and green. Among the SiO_2-NP-treated groups, the 15-nm treatment had more significant effects than the 50-nm treatment. Interestingly, the 15-nm 1000 μg/mL group and the 50-nm 300 μg/mL group exhibited similar changes in their swimming path patterns and locomotive activities. The effects of nanoparticle size and concentration were obvious, with a small particle size (15-nm) and higher concentration (1000 μg/mL) exerting stronger effects.

To explore the precise effects of SiO_2-NPs on instantaneous locomotive activities at each location in the swimming path over the

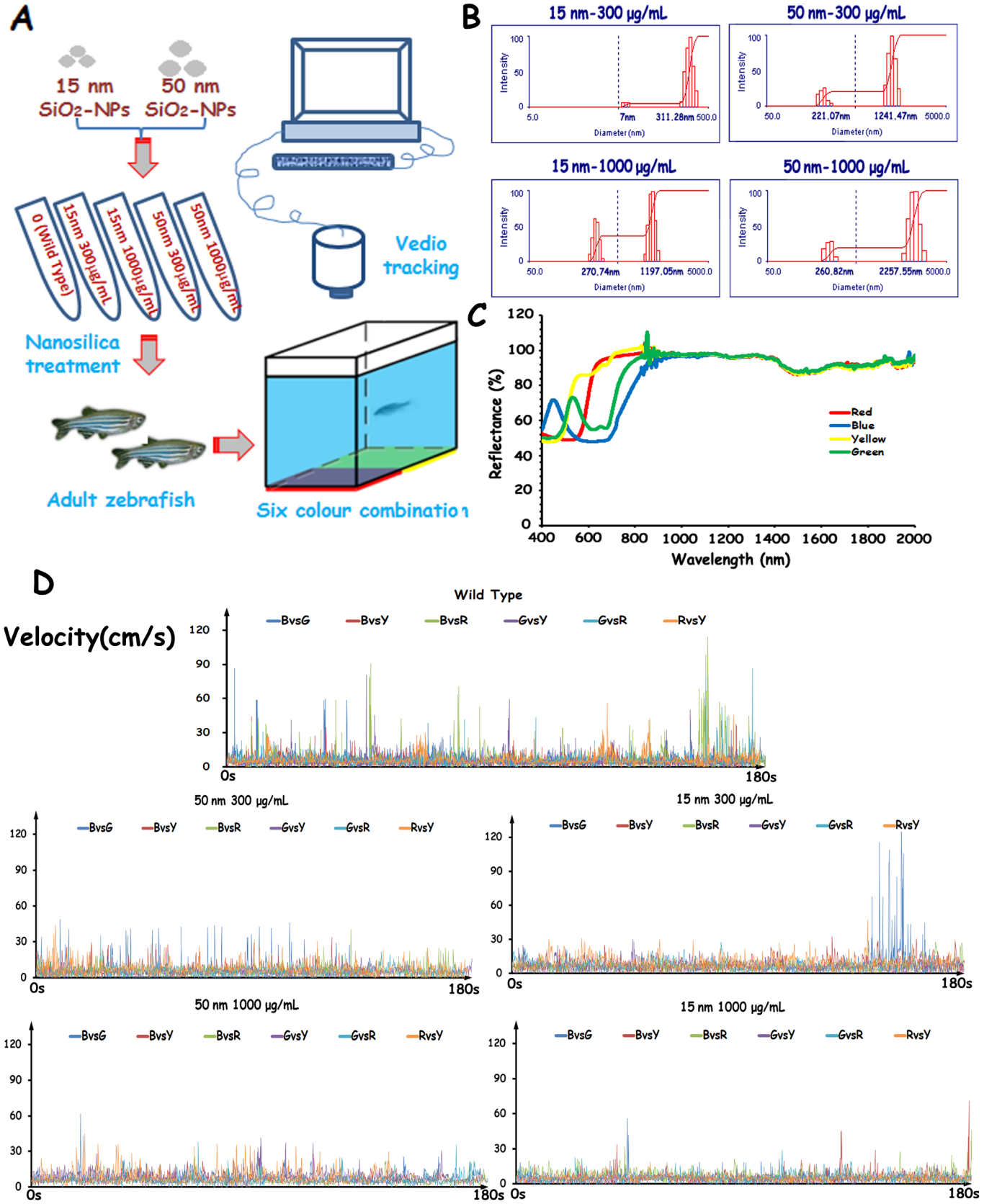

Figure 1 | Behavioural experimental procedures and properties of nanosilica and colour. (A) A schematic of the nanosilica treatment and behavioural tests recorded in adult zebrafish using video tracking. (B) Characterisation of nanosilica dispersed in a standard water system using dynamic light scattering (DLS). (C) Characterisation of four colours applied in a colour preference test using a UV-VIS-NIR spectrophotometer. (D) Representative sequence chart of the velocity parameter of adult zebrafish tested in a CPP apparatus.

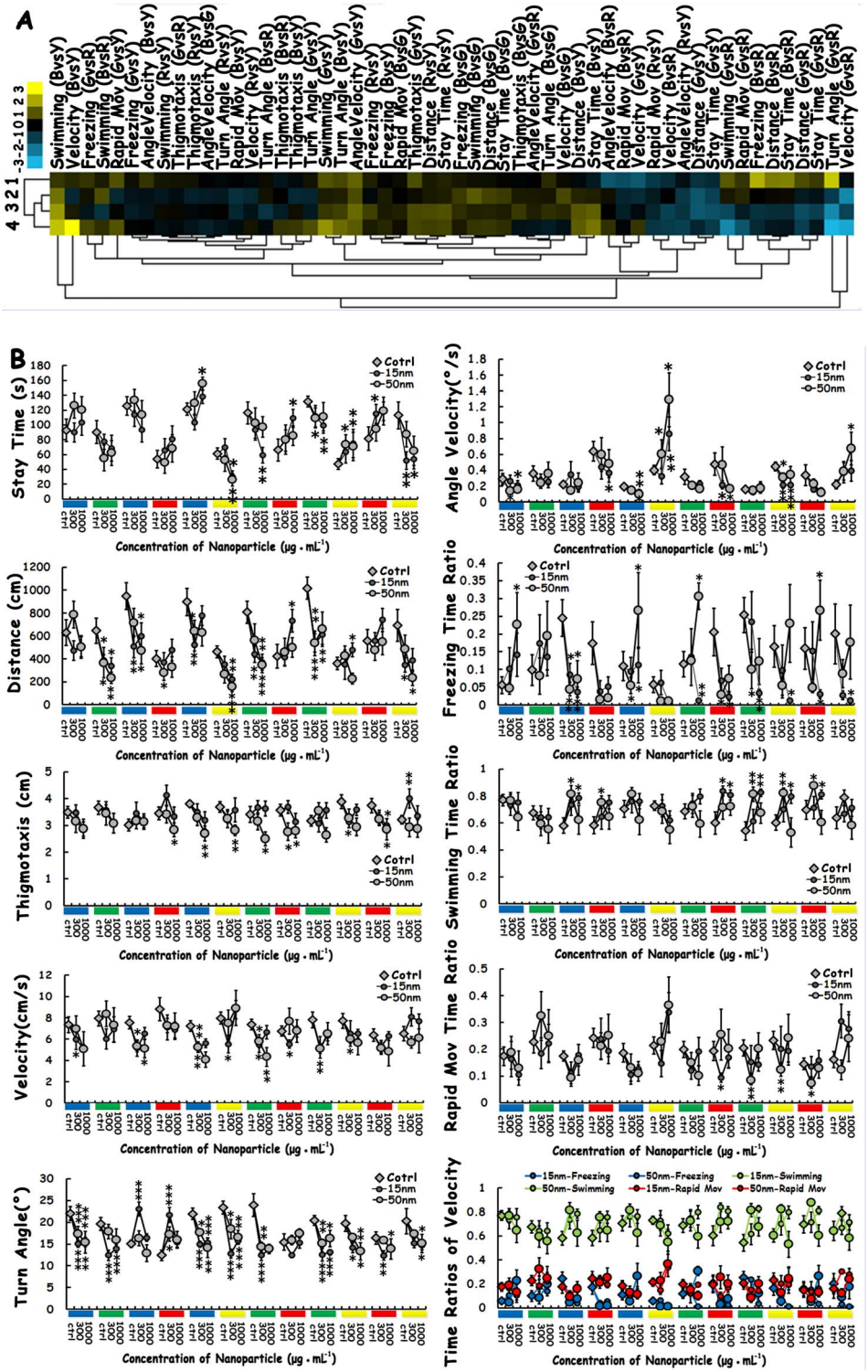

Figure 2 | Behavioural phenotyping of behavioural changes induced by SiO_2-NPs. (A) Clustering analyses were performed on the data from the entire 18 min test in six colour combinations; all the behavioural parameters, including colour preference and locomotive activity, and the four different sizes and concentrations were included in the analyses. In the clustergram, each cell represents the average relative value and in terms of the standard deviation for each behavioural parameter (blue = lower than control; yellow = higher than control; and black = invariable). The numeral "1" represents the 15-nm 300 μg/mL group, "2" represents the 50-nm 300 μg/mL group, "3" represents the 15-nm 1000 μg/mL group, and "4" represents the 50-nm 1000 μg/mL group. (B) Statistical analysis of the effects of size and concentration on each individual colour preference behavioural parameter in six colour combinations (12 colour lumps). In each line chart, six different colour combinations (12 colour lumps) a located under the x-axis, representing the different colours beneath the CCP compartments in the experimental condition. The three scales located under each colour lump indicate the three different SiO_2-NP concentrations (0, 300 μg/mL and 1000 μg/mL) at which the zebrafish were treated. As shown in the legend for each line chart, the hollow diamonds represent the wild-type zebrafish, the small, solid black balls represent the SiO_2-NPs with a 15-nm diameter, and the slightly larger hollow balls represent the SiO_2-NPs with a 50-nm diameter. The asterisks represent significant differences between the SiO_2-NP-treated and wild-type fish, with an asterisk close to the 15-nm (or 50-nm) balls indicating a significant difference between the 15-nm-treated (or 50-nm treated) and wild-type zebrafish. The data represent the means ± SEM of n = 12 zebrafish. *$p < 0.05$, **$p < 0.01$, ***$p < 0.001$.

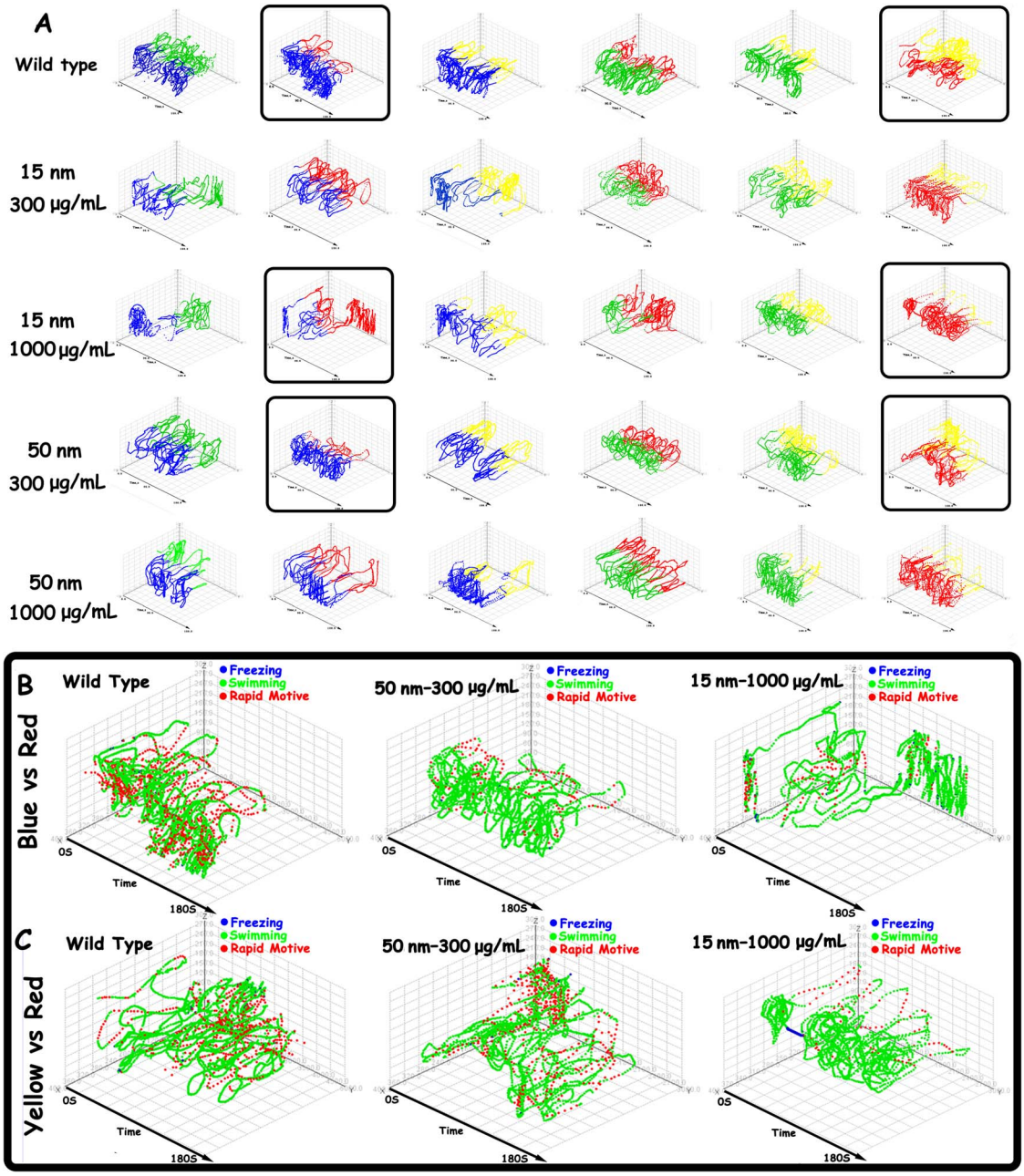

Figure 3 | Spatiotemporal behavioural phenotyping of all behavioural changes induced by SiO_2-NPs. (A) Reconstructed spatiotemporal swimming path changes in six colour combinations induced by nanosilica of different sizes and concentrations. The coloured path represents the swimming path followed by the zebrafish that corresponds to the coloured compartment in CPP. (B) Locomotion (mobility) differences between zebrafish in the wild-type, 50-nm 300 μg/mL and 15-nm 1000 μg/mL groups in the blue vs. red combination. (C) Locomotion (mobility) differences between zebrafish in the wild-type, 50-nm 300 μg/mL and 15-nm 1000 μg/mL groups in the yellow vs. red combination.

course of 180 s, we colour-coded the locomotive activities; the legend colour scales represent the proportional spectrum across the minimum/maximum ranges of the locomotive parameter values (Supplementary Figures S6–11). The swimming velocity pattern was selected to demonstrate that SiO_2-NPs decreased the instantaneous velocity of adult zebrafish. Based on the clustering results, SiO_2-NPs at 15-nm 1000 μg/mL and 50-nm 300 μg/mL produced similar changes in the behavioural patterns of zebrafish. The behavioural statistical analyses showed that SiO_2-NPs increased the preference for the red colour. Thus, the 15-nm 1000 μg/mL and 50-nm 300 μg/mL groups and the red vs. blue and red vs. yellow combinations were selected to demonstrate the spatiotemporal changes in locomotive activities. Specifically, Fig. 3B, C shows the spatiotemporal velocity distribution of the patterns of the wild-type, 15-nm 1000 μg/mL treated and 50-nm 300 μg/mL treated zebrafish. The wild-type zebrafish demonstrated high locomotive activities, with an intense, rapid motive swimming position (red point), a homogeneously distributed swimming position (green point) and a rare freezing point (blue point). In contrast, the SiO_2-NP-treated zebrafish exhibited a decrease in robust motions, a reluctance to swim rapidly and a tendency to wander slowly. The 15-nm 1000 μg/mL treatment significantly decreased the rapid motive point and increased the freezing point.

The effects of SiO_2-NP treatment on the retina and brain of zebrafish. Because treatment with SiO_2-NPs disturbed colour preference in the zebrafish, we examined the expression of Zpr-1 by labelling cone cells, the photoreceptors responsible for colour vision in the

zebrafish retina[31]. As shown in Fig. 4, there was the expression level of Zpr-1 did not differ between the wild-type group and the SiO_2-NP-treated groups. The monoclonal antibody (mAb) Zpr-1 specifically labels an antigen associated with the plasma membrane of double cone cells[32]; thus, mAb Zpr-1 can be used to label the morphology of cone cells. Compared with the wild-type group, the four SiO_2-NP-treated groups exhibited abnormal morphology in the cone cells of the retina.

SiO_2-NP treatment of zebrafish in CPP tanks can lead to decreased locomotive activity and abnormal motion patterns, which are characteristic behaviours of Parkinson's disease[23]. Parkinson's disease results from the progressive loss of DA cells in the substantia nigra. To study whether the observed decrease in locomotive activity was related to a loss of DA cells, the expression of tyrosine hydroxylase (TH) was examined by immunohistochemistry and western blotting. The results showed that SiO_2-NP treatment decreased the expression of TH in the posterior tuberculum (TP) and substantia nigra of the zebrafish[33]. The levels of TH in the groups treated with 15-nm 300 μg/mL and 15-nm 1000 μg/mL were much lower than in the wild-type group.

In addition, we performed HE staining to examine the histopathology of the brain and retina in zebrafish after 7 days of exposure to SiO_2-NPs. No apparent changes in the histology of the brain or retina were observed in the groups that received SiO_2-NP treatment compared with the wild-type group.

Discussion

In this study, we tested the neurotoxic effects of different sizes (15-nm and 50-nm) and concentrations (low: 300 μg/mL and high: 1000 μg/mL) of silica nanoparticles. Treatment with SiO_2-NPs 15-nm in size and 300 μg/mL in concentration produced the most significant effects on all the tested parameters (general, cognitive behaviour and locomotive activity). These findings highlight the significant role of small particle size in neurotoxic effects. Furthermore, nanosilica, especially 15-nm SiO_2-NPs, disrupted the advanced learning and memory cognitive behaviours that are inherent to zebrafish. In terms of colour preference, SiO_2-NPs significantly increased the degree of preference for the colour red, which plays a critical role in the behaviour and ecology of zebrafish. Moreover, silica, especially 15-nm SiO_2-NPs, decreased the degree of locomotive activity and the normal kinetic pattern of the zebrafish in the CPP tank, resulting in behaviours similar to those observed in neurodegenerative diseases. Furthermore, the 3D spatiotemporal reconstruction of the SiO_2-NP-treated zebrafish confirmed the neurodegenerative behaviour pattern induced by SiO_2-NPs. In conclusion, small SiO_2-NPS were more neurotoxic than larger SiO_2-NPs and exerted their effects by either changing cognitive behaviours or introducing neurodegenerative behaviour in zebrafish.

The deviation of the colour preference parameters from the normal values and the changes in the swimming path of the zebrafish treated with SiO_2-NPs demonstrated that SiO_2-NP treatment could disturb the natural mode of colour preference in adult zebrafish. Similar to the human retina, the zebrafish retina is highly organised neural tissue, and the retinal photoreceptors are the primary sensory cells responsible for detecting light. The zebrafish retina contains both rod and cone photoreceptor cells. Rod photoreceptor cells mediate dim-light and night vision, whereas cone photoreceptor cells are responsible for mediating day-time bright light and colour vision. In our study, cone photoreceptor cells were labelled with mAb Zpr-1 to determine whether SiO_2-NP treatment could disturb the natural mode of colour preference; no differences in the expression level of Zpr-1 were found between the wild-type group and the SiO_2-NP-treated groups. However, the retinas of the four SiO_2-NP-treated groups exhibited abnormal cone cell morphology, especially in the outer segments. The outer segment contains stacked membranous discs that harbour the components of the phototransduction apparatus[34,35]. The histopathological features of the retinas of the SiO_2-NP-treated zebrafish were also examined by HE staining; no difference was detected between the wild-type group and the treated groups. Together, these data suggest that the disturbed colour preference exhibited by the four SiO_2-NP-treated zebrafish groups was likely due to a cone photoreceptor defect, which may have been caused by the SiO_2-NPs; this type of treatment is known to damage phototransduction.

SiO_2-NP treatment results in decreased locomotive activity in zebrafish, which is evidenced by decreased locomotive parameters (such as distance, velocity and freezing time ratio) and the 3D spatiotemporal reconstruction of the swim path. It has been reported that decreased locomotive activity is the primary representative behavioural alteration exhibited by the zebrafish model of Parkinson's disease[23]. Parkinson's disease is characterised by the progressive loss of DA neurons in the substantia nigra[23]. In the SiO_2-NP-treated zebrafish, the DA neurons labelled by the TH antibody were reduced in the posterior tuberculum (PT), the counterpart of the substantia nigra of amniotes. Together, the data suggest that SiO_2-NP treatment could induce the characteristics of Parkinson's disease in zebrafish. They also suggest that the decreased locomotive activity observed in the treated zebrafish was caused, at least in part, by the loss of DA cells in the posterior tuberculum. The four groups of zebrafish treated with SiO_2-NPs of different sizes and concentrations exhibited DA cell loss to different extents, which may be the reason for the variations in the degree to which their locomotive activity was decreased.

Methods

Experimental animals. All the experimental protocols and procedures involving zebrafish were approved by the Committee for Animal Experimentation of the College of Life Science at Nankai University (no. 2008) and were performed in accordance with the NIH Guide for the Care and Use of Laboratory Animals (no. 8023, revised in 1996). The animals were maintained in aquaria at 28.5°C with a 10/14 h dark/light cycle.

Zebrafish exposed to SiO_2-NPs. The zebrafish were maintained in regular tank water (KCl 0.05 g L^{-1}, $NaHCO_3$ 0.025 g L^{-1}, NaCl 3.5 g L^{-1} and $CaCl_2$ 0.1 g L^{-1}, pH 7.0–7.2) and were fed live brine shrimp twice per day. The fish were separated into three groups, each consisting of 12 adult zebrafish. The three groups were exposed to tank water (as a control), 300 μg/mL SiO_2-NPs or 1000 μg/mL SiO_2-NPs in 3 L system tanks for 7 days before the conditioned preference place (CPP) tank test.

Apparatus for the CPP tank test. The colour preference behaviour and locomotive activities of the zebrafish treated with nanosilica were observed in the CPP apparatus[27], which consisted of a two-chambered PP box (23 × 15 × 15 cm) containing 12 cm of water (from the bottom). To test the colour preference behaviour of the zebrafish, the CPP tank was slightly modified: the black dots on one side of the bottom were replaced with different coloured paper.

Behavioural parameters for colour preference. Stay time was defined as the absolute duration of time spent on each coloured side during a 3-min period. More time spent on one coloured side indicated a preference for this colour. **Distance** was defined as the total swimming length (cm) of the zebrafish on each coloured side during the 3-min test for each colour combination. A high value for this parameter on one coloured side indicated a preference for that colour. A lower distance value was interpreted as a zebrafish demonstrating neurodegenerative disease-like behaviours. **Thigmotaxis** was defined as the mean distance (cm) of the fish from the nearest wall in each coloured side of the CPP tank, with lower values indicating a higher preference for the colour on the side of the CPP tank.

Behavioural parameters for locomotive activity. Distance was also considered a locomotive parameter and was defined the same way as decribed above in behavioural parameters for colour preference. Velocity was calculated as the total path length (cm), divided by the test duration in seconds (180 s). **Turn angle** was defined as the mean angle created by three adjacent samples and averaged across all the samples. **Angle velocity** was calculated as the sum of the values for all the transient angles divided by 180 s. **Freezing time ratio** was calculated as the absolute length of time during which the transient velocity of the zebrafish was less than 1 cm/s, divided by the total test duration in seconds (180 s). **Swimming time ratio** was calculated as the absolute length of time during which the transient velocity of the zebrafish was between 1 cm/s and 10 cm/s, divided by the test duration in seconds (180 s). **Rapid movement time ratio** was calculated as the absolute length of time during which the transient velocity of the zebrafish was greater than 10 cm/s, divided by the total test duration in seconds (180 s).

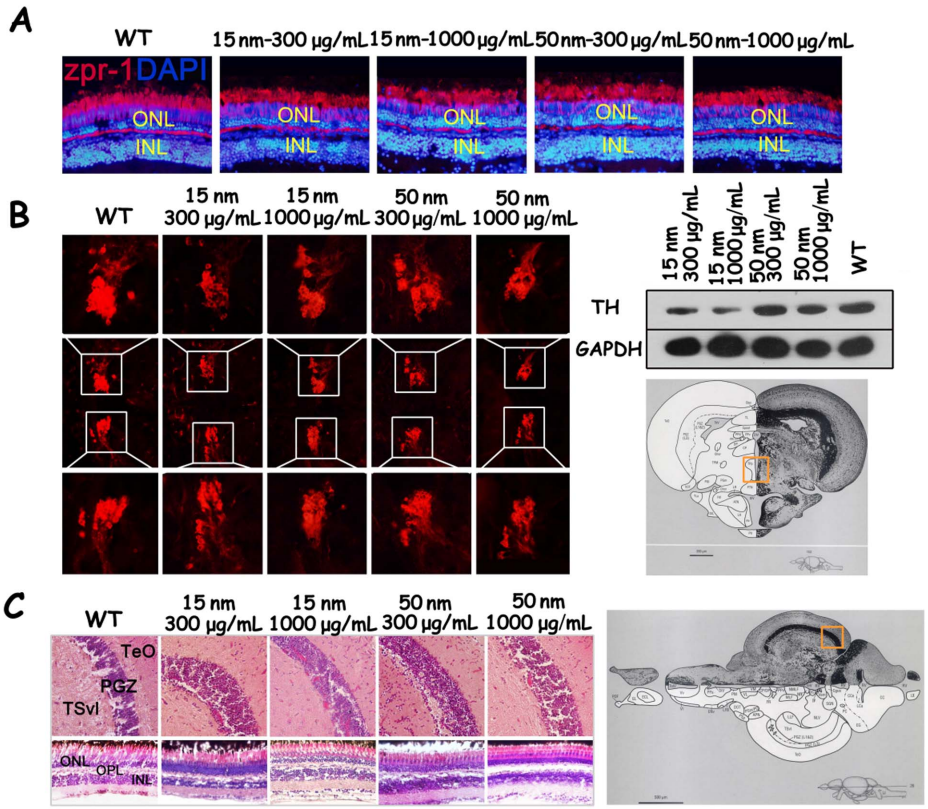

Figure 4 | The effects of SiO_2-NP treatment on the retina and brain of zebrafish. (A) Cone photoreceptor cells labelled by the Zpr-1 antibody in wild-type zebrafish and zebrafish groups treated with SiO_2-NPs. (B) Tyrosine hydroxylase expression in the posterior tuberculum (TP) (measured by immunohistochemistry) and in the brain (measured by western blotting). (C) The histopathology of the brain and retina in wild-type zebrafish and in the groups treated with SiO_2-NPs. ATN, anterior tuberal nucleus. Chor, commissura horizontalis. CP, central posterior thalamic nucleus. Cpost, commissural posterior. Ctec, commissural tecti. DIL, diffuse nucleus of the inferior lobe. DiV, diencephalic ventricle. DP, dorsal posterior thalamic nucleus. FR, fasciculus retroflexus. Hd, dorsal zone of periventricular hypothalamus. Hv, ventral zone of periventricular hypothalamus. LH, lateral hypothalamic nucleus. LR, lateral recess of diencephalic ventricle. PGI, lateral preglomerular nucleus. PGm, medial preglomerular nucleus. PGZ, periventricular gray zone of optic tectum. Pit, pituitary. PPd, periventricular pretectal nucleus, dorsal part. PPv, periventricular pretectal nucleus, verntal part. PTN, posterior tuberal nucleus. TeO, tectum opticum. TeV, tectum ventricle. TL, torus longitudinalis. TLa, torus lateralis. TPM, trcatus pretectomamillaris. TPp, periventricular nucleus of posterior tuberculum. VOT, ventrolateral optic tract.ONL, outer nuclear layer. INL, inner nuclear layer. APN, accessory pretectal mucleus. CC, crista cerebellaris. CCe, corpus cerebelli. Cgus, commissure of the secondary gustatory nuclei. DOT, dorsomedial optic tract. ECL, external cellular layer of olfactory bulb including mitral cell. EG, eminetia granularis. ENv, entopenduncular nucleus, vertral part. GC, griseum centrale. GL, glomerular layer of olfactory bulb. LCa, lobus caudalis cerebelli. LFB, lateral forebrain bundle. LLF, lateral longitudinal fascicle. LX, vagal lobe. MLF, medial longitudinal fascicle. NLV, nucleus lateralis valvulae. NMLF, nucleus of the medial longitudinal fascicle. NIV, trochlear nucleus. PC, posterior cerebellar tract. PM, magnocellular preoptic nucleus. PO, posterior pretectal nucleus. POF, primary olfactory fiber layer. PPa, periventricular pretectal nucleus, anterior part. PSm, magnocellular superficial pretectal nucleus. PSp, parvocellular superficial pretectal nucleus. RV, rhombencephalic ventricle. SGN, secondary gustatory ventricle. TelV, telencephalic ventricles. TSvl, ventrolateral nucleus of torus semicircularis. V, ventral telencephalic area. Vam, medial division of valvula cerebelli. VI, lateral nucleus of V. VL, ventrolateral thalamic mucleus. VM, ventromedial thalamic nucleus. Vv, ventral nucleus of V. IV, trochlear nerve. Cropped blots are used in the figure. Full-length blots are presented in Supplementary Figure S12. The images of zebrafish brain atlas in parts B and C are reproduced from Wullimann, M., *Neuroanatomy of the Zebrafish Brain: A topological atlas*, Birkhauser press, Basel (1996)[36], chapter 5 figure 153 and chapter 5 figure 26, respectively, with kind permission from Springer Science and Business Media.

Behavioural experiments. The behavioural experimental procedures are illustrated in Supplementary Figure S3. Details of the pre-test training procedure for the zebrafish were provided in a previous work[27]. Each group consisted of 12 adult zebrafish that were maintained and treated in a 3 L tank for 7 days. Two types of SiO_2-NPs of different sizes were applied to the adult zebrafish as treatments. The adult zebrafish were divided into the five following treatment groups: tank water (as a control), nanosilica at a size of 15-nm and a concentration of 300 μg/mL, 15-nm 1000 μg/mL nanosilica, 50-nm 300 μg/mL nanosilica or 50-nm 1000 μg/mL nanosilica. Beginning on the second day of the 7 day period, all the fish were initially trained in accordance with their group in the CPP apparatus. To ensure that they became aware of the existence of the two different compartments in the CPP apparatus, "the fish were habituated to the CPP with a transparent perforated barrier in the middle of the apparatus; this impeded movement between the compartments. For each dosed group, 12 fish were initially trained in the CPP, and the number of fish was halved after the shoal had explored all the compartments; the fish were given four min to explore the CPP during each session. Finally, we ensured that each fish had explored all the compartments singly.

On the eighth day, when all the fish had been dosed and adapted to the CPP apparatus for 7 days, a colour preference test was performed. We tested six different combinations of four colours (red and yellow; red and green; red and blue; yellow and green; yellow and blue; and green and blue). Paper of one colour was attached to the bottom of one chamber, and a different colour paper was attached to the bottom of the other chamber. During the 3 min test, each fish was tested individually, and its movement was tracked by a video camera for computer analysis. We evaluated the behavioural parameters (including the swimming path) of the zebrafish via self-designed software for zebrafish tracking; the accuracy and availability of the software is described in the supporting material (Supplementary Figures S1–2). Nine behavioural endpoints were analysed statistically to determine the effects of nanosilica on the cognitive and locomotive behaviours of the dosed zebrafish. Details of the experimental procedures and the behavioural and physiological analyses are provided

in Supplementary Figure S4. The characterisation of the nanoparticles of different sizes and concentrations, as well as the colours used in this research, are described in Fig. 1B and Supplementary Table S1.

Preparation, characterisation, and stability of SiO_2-NPs in system water. The SiO_2-NPs (15-nm and 50-nm) employed in our experiment were purchased from Xuan Cheng Jing Rui New Material Co., Ltd. (China). Before being suspended in a 3-L tank, SiO_2-NPs of different sizes and concentrations were prepared by weighing and adding dry powder NPs (15-nm and 50-nm) to system water. The amount of silica particles added corresponded to the experimental group (0, 300 μg/mL or 1000 μg/mL). To facilitate the suspension of the particles, the solutions were sonicated for 30 min. The diameters and distributions of the 15-nm and 50-nm nanosilica in the system water were then determined using dynamic light scattering (DLS).

Immunohistochemistry. After the adult zebrafish had been exposed to the treatments for 7 days, their eyes and brain tissues were harvested and immediately fixed in 4% paraformaldehyde, equilibrated in 30% sucrose/PBS overnight and embedded in OCT. Sections of 12 μm thickness were mounted on gelatin-coated slides and air dried at 37°C for at least 2 h. The tissue sections were rehydrated with PBS, blocked with 20% NGS and 2% BSA in 0.3% PBS/Triton X-100 (PBST) for 1 h and incubated with primary antibodies overnight at 4°C. The following primary antibodies and concentrations were used: mouse monoclonal antibody Zpr-1 (1 : 200, University of Oregon) for labelling cones and mouse monoclonal anti-tyrosine hydroxylase (1 : 400, Millipore, Billerica, MA) for labelling DA cells. The interpretation of neuroanatomy follows the adult zebrafish brain atlas[36]. Immunoreactions were detected using Cy3-labelled goat anti-mouse IgG diluted to 1 : 400 (Millipore). The sections were counterstained with a 1 : 1000 dilution of 4',6-diamidino-2-phenylindole (DAPI) (Sigma) to label the nuclei. The slides were viewed with an Olympus BX51 light microscope (Olympus, Tokyo, Japan). The images obtained by an Olympus CCD DP71 (Olympus) were processed using Adobe Photoshop CS (Adobe Systems, San Jose, CA).

Histopathological examination. After the adult zebrafish had been exposed to the treatments for 7 days, their eyes and brain tissues were harvested and immediately fixed in 4% paraformaldehyde. The tissues were processed routinely for paraffin embedding, and 8-μm-thick sections were cut and mounted onto glass slides. The tissue samples were stained with haematoxylin and eosin. The sections were evaluated and photographed using an Olympus BX51 light microscope equipped with an Olympus CCD DP71 (Olympus).

Western blot analysis. The level of tyrosine hydroxylase protein in the zebrafish brain was detected by western blot analysis. After exposure for 7 days, the brains of adult zebrafish were harvested and immediately lysed in a tissue protein extraction reagent (CWBIO, Beijing, China) and 5 μL PMSF (Sigma-Aldrich). The protein concentrations were quantified using the BCA Protein Assay Kit (CWBIO). The proteins were subjected to SDS-PAGE and transferred onto a nitrocellulose membrane blocked with 5% non-fat dry milk in Tris-buffered saline with 0.05% Tween-20. The membrane was incubated with the following primary antibodies: mouse anti-TH (1 : 1000; Millipore) and mouse anti-GAPDH (1 : 5000; Abmart, Shanghai, China). After being washed with Tris-buffered saline containing 0.05% Tween-20, the membrane was incubated with an anti-mouse peroxidase-conjugated secondary antibody (1 : 3000; CWBIO). The membrane was then washed with Tris-buffered saline containing 0.05% Tween-20, and the Super Signal West Pico chemiluminescent substrate (Thermo Scientific) was used for detection.

Data analysis. *Statistical analysis.* To compare the same behavioural endpoint in different-coloured compartments in the CPP test, a two-sample heteroscedasticity hypothesis t-test was performed using Excel 2013. Significance was set at $p < 0.05$ for all the experiments. All the results are presented as the means ± standard error of the mean (SEM).

Cluster analysis. This study employed cluster analysis as an unsupervised statistical method to assess the effects of SiO_2-NPs of different sizes (15-nm and 50-nm) and concentrations on various behavioural parameters of fish based on similarities between their behavioural alterations[37]. Cluster 3.0 (Stanford University, USA) was used to perform hierarchical clustering ordered by Euclidean distances to link the sizes and concentrations of nanosilica to the behavioural parameters of the zebrafish. The clustering results were visualised as a dendrogram and a coloured array in Java Tree View (University of Glasgow, UK). The data used for the clustering analysis included the colour preference behavioural parameters and the locomotive activity parameters. The experimental results were hierarchically clustered to link the SiO_2 treatments to the observed behaviours (based on the behavioural endpoints listed above, generated via the vertical angle of view video-tracking using self-designed zebrafish tracking software). In the clustergram, each cell represents the average relative value and the standard deviation (blue = lower than the control, red = higher than the control, and black = invariable) for each behavioural endpoint.

3D spatiotemporal reconstruction of swim path demonstration. 3D spatiotemporal reconstructions permit rapid and objective macro- and micro-level behavioural analyses, thereby improving high-throughput phenotyping of zebrafish behaviour[38]. To evaluate the effects of SiO_2-NPs of different sizes (15-nm and 50-nm) and concentrations on the spatial movement of the zebrafish in the CPP tank, a 3D spatiotemporal reconstruction of the swim path was created using the Rapid Miner 5.0 software. The procedure used to generate the 3D spatiotemporal reconstruction of the swim path was previously described in detail[38]. Each reconstructed swim path was obtained from a zebrafish tested in the CPP apparatus for 3 min following 7 days of continuous exposure to SiO_2-NPs of different sizes and concentrations. The 3D spatiotemporal swim path pictures were derived from the plane swimming trajectory in two dimensions (X- and Z-axes) and were tracked by a camera pointing on the timeline (Y-axis). As shown in Fig. 3A, for each zebrafish, a 3D spatiotemporal swim path was generated to detect the effects of the size and concentration of the SiO_2-NPs on the swim path pattern of the treated zebrafish. The X- and Z-axes represent the zebrafish plane swimming path, and t (Y-axis) represents the 3 min test time. A different-coloured swimming path represents the trail of motion in the corresponding colour compartment in the CPP.

For each experiment, the raw tracking data were obtained from the self-designed zebrafish tracking software, exported into Excel spreadsheets and subsequently imported into Rapid Miner 5.0 to create 3D spatiotemporal swim path reconstructions, as previously described in detail[39,40]. We also used Rapid Miner 5.0 software to integrate the spatiotemporal (X, Z, time) coordinates, colour preference parameters and motive parameters into a single track file. We used the X- and Z-coordinates and time (Y-axis) to construct the 3D temporal coloured swim path in the corresponding coloured compartment. A detailed dissection of the behavioural endpoints as episodes with changing colour indicating variability in the behavioural parameter values was performed to determine the spatial and temporal variations and the distribution patterns of the behavioural parameters of the locomotive activities.

1. Lin, Y. S. & Haynes, C. L. Impacts of mesoporous silica nanoparticle size, pore ordering, and pore integrity on hemolytic activity. *J. Am. Chem. Soc.* **132**, 4834–4842 (2010).
2. Bottini, M. *et al.* Quantum dot-doped silica nanoparticles as probes for targeting of T-lymphocytes. *Int. J. Nanomedicine.* **2**, 227–233 (2007).
3. Hirsch, L. R. *et al.* Nanoshell-mediated near-infrared thermal therapy of tumors under magnetic resonance guidance. *Proc. Natl Acad. Sci. USA.* **100**, 13549–13554 (2003).
4. Slowing, I. I., Trewyn, B. G. & Lin, V. S. Mesoporous silica nanoparticles for intracellular delivery of membrane-impermeable proteins. *J. Am. Chem Soc.* **129**, 8845–8849 (2007).
5. Bharali, D. J. *et al.* Organically modified silica nanoparticles: a nonviral vector for in vivo gene delivery and expression in the brain. *Proc. Natl Acad. Sci. USA.* **102**, 11539–11544 (2005).
6. Boxall, B. A. A., Tiede, C. & Chaudhry, Q. Engineered nanomaterials in soils and water: how do they behave and could they pose a risk to human health? *Int. J. Nanomedicine.* **2**, 919–927 (2007).
7. Wang, J. *et al.* Expression changes of dopaminergic system-related genes in PC12 cells induced by manganese, silver, or copper nanoparticles. *Neurotoxicology.* **30**, 926–933 (2009).
8. Lockman, P. R. *et al.* Nanoparticle surface charges alter blood-brain barrier integrity and permeability. *J. Drug Target.* **12**, 635–641 (2004).
9. Kashiwada, S. Distribution of nanoparticles in the see-through medaka (oryzias latipes). *Environ Health Persp.* **114**, 1697–1702 (2006).
10. Wu, J., Wang, C., Sun, J. & Xue, Y. Neurotoxicity of silica nanoparticles: brain localization and dopaminergic neurons damage pathways. *ACS nano.* **5**, 4476–4489 (2011).
11. Schafer, D. P. *et al.* Microglia sculpt postnatal neural circuits in an activity and complement-dependent manner. *Neuron.* **74**, 691–705.
12. Deleidi, M. & Isacson, O. Viral and Inflammatory triggers of neurodegenerative diseases. *Sci. Transl. Med.* **4**, 121–124 (2012).
13. Groth, C. *et al.* Identification of a second presenilin gene in zebrafish with similarity to the human alzheimer's disease gene presenilin 2. *Dev. genes. Evol.* **212**, 486–490 (2002).
14. Nornes, S. *et al.* Developmental control of Presenilin1 expression, endoproteolysis, and interaction in zebrafish embryos. *Exp Cell Res.* **289**, 124–132 (2003).
15. Nornes, S. *et al.* Independent and cooperative action of Psen 2 with Psen 1 in zebrafish embryos. *Exp Cell Res.* **315**, 2791–2801 (2009).
16. Newman, M. *et al.* Altering presenilin gene activity in zebrafish embryos causes changes in expression of genes with potential involvement in Alzheimer's disease pathogenesis. *J. Alzheimer's Dis.* **16**, 133–147 (2009).
17. Joshi, P. *et al.* Amyloid precursor protein is required for convergent-extension movements during zebrafish development. *Dev. Biol.* **335**, 1–11 (2009).
18. Musa, A., Lehrach, H. & Russo, V. E. Distinct expression patterns of two zebrafish homologues of the human APP gene during embryonic development. *Dev. Genes Evol.* **211**, 563–567 (2001).
19. Babin, P. J. *et al.* Both apolipoprotein E and AI genes are present in a nonmammalian vertebrate and are highly expressed during embryonic development. *Proc. Natl Acad. Sci. USA.* **94**, 8622–8627 (1997).
20. Campbell, W. A. *et al.* Zebrafish lacking Alzheimer presenilin enhancer 2 (Pen-2) demonstrate excessive p53-dependent apoptosis and neuronal loss. *J. Neurochem.* **96**, 1423–1440 (2006).
21. Zetterberg, H. *et al.* The cytosolic loop of the γ-secretase component presenilin enhancer 2 protects zebrafish embryos from apoptosis. *J. Bio. Chem.* **281**, 11933–11939 (2006).

22. Chen, M., Martins, R. N. & Lardelli, M. Complex splicing and neural expression of duplicated tau genes in zebrafish embryos. *J. Alzheimer's Dis.* **18**, 305–317 (2009).
23. Bretaud, S., Lee, S. & Guo, S. Sensitivity of zebrafish to environmental toxins implicated in Parkinson's disease. *Neurotoxicol Teratol.* **26**, 857–864 (2004).
24. Schiffer, N. W. *et al.* Identification of anti-prion compounds as efficient inhibitors of polyglutamine protein aggregation in a zebrafish model. *J. Bio Chem.* **282**, 9195–9203 (2007).
25. Lumsden, A. L. *et al.* Huntingtin-deficient zebrafish exhibit defects in iron utilization and development. *Hum. Mol. Genet.* **16**, 1905–1920 (2007).
26. Miller, V. M. *et al.* CHIP suppresses polyglutamine aggregation and toxicity in vitro and in vivo. *J. Neuro Sci.* **25**, 9152–9161 (2005).
27. Avdesh, A. *et al.* Evaluation of color preference in zebrafish for learning and memory. *J. Alzheimers Dis.* **28**, 459–469 (2012).
28. Xue, J. Y. *et al.* An assessment of the impact of SiO_2 nanoparticles of different sizes on the rest/wake behavior and the developmental profile of zebrafish Larvae. *Small.* **9**, 3161–3168 (2013).
29. Hughes, A. *et al.* Cone contributions to the photopic spectral sensitivity of the zebrafish ERG. *Visual Neurosci.* **15**, 1029–1037 (1998).
30. Spence, R. & Smith, C. Innate and learned colour preference in the zebrafish, *Danio rerio Ethology*. **114**, 582–588 (2008).
31. Brockerhoff, S. E. & Fadool, J. M. Genetics of photoreceptor degeneration and regeneration in zebrafish. *Cell and Mol Life Sci.* **68**, 651–659 (2011).
32. Larison, K. D. & Bremiller, R. Early onset of phenotype and cell patterning in the embryonic zebrafish retina. *Development.* **109**, 567–576 (1990).
33. Rink, E. & Wullimann, M. F. The teleostean (zebrafish) dopaminergic system ascending to the subpallium (striatum) is located in the basal diencephalon (posterior tuberculum). *Brain Res.* **889**, 316–330 (2001).
34. Tsujikawa, & Malicki, J. Genetics of photoreceptor development and function in zebrafish. *Int J Dev Biol.* **48**, 925–934 (2004).
35. Reynolds, A. L. The genetics of outer segment morphogenesis in zebrafish. *Retinal degenerative diseases.* **723**, 431–441. Springer press, New York (2012).
36. Wullimann, M. *Neuroanatomy of the Zebrafish Brain:a topological atlas* Wullimann, M. (ed.). **38**, 83. Birkhauser press, Basel (1996).
37. Shannon, W., Culverhouse, R. & Duncan, J. Analyzing microarray data using cluster analysis. *Pharmacogenomics.* **4**, 41–52 (2003).
38. Cachat, J. *et al.* Three-dimensional neurophenotyping of adult zebrafish behavior. *PLoS ONE.* **6**(3): p. e17597. doi:10.1371/journal.pone.0017597 (2011).
39. Cachat, J. Video-aided analysis of zebrafish locomotion and anxiety-related behavioral responses. *Zebrafish Neurobehavioral Protocols*. Kalueff, A. (ed.), 1–14. Springer press, New York (2011).
40. Cachat, J. Deconstructing adult zebrafish behavior with swim trace visualizations. *Zebrafish Neurobehavioral Protocols*. Kalueff, A. (ed.). 191–201. Springer press, New York (2011).

Acknowledgments

This project was initiated in the State Key Laboratory of Medicinal Chemical Biology at Nankai University. X.Z., D.Y.C. and X.Z.F. were supported by the Special Fund for Basic Research on Scientific Instruments of the Chinese National Natural Science Foundation (grant no: 61327802). The work performed in the laboratory of X.Z.F. was supported by the National Natural Science Foundation of China (grant no: 81071260). The work performed by the group of D.Y.C. was supported by the Tianjin Science Technology Research Funds of China (grant no: 10JCYBJC25300). And the fund from the State Key Laboratory of Medicinal Chemical Biology (grant no: 20130301).

Author contributions

X.Z.F. conceived the idea of the study. X.L. designed the experiments. X.L. and Y.X.L. conducted the zebrafish behavioural experiments. B.L., X.Z. and M.Z.S. designed the zebrafish video tracking software. X.L., B.L. and M.Z.S. performed the data mining and analysis. X.L.L. and D.Y.C. performed the histological, cellular and molecular experiments. X.L. wrote the majority of the manuscript; D.Y.C. wrote the histological, cellular and molecular sections, and B.L. wrote the video tracking software design section.

Additional information

Supplementary information accompanies this paper at http://www.nature.com/scientificreports

Competing financial interests: The authors declare no competing financial interests.

How to cite this article: Li, X. *et al.* SiO_2 nanoparticles change colour preference and cause Parkinson's-like behaviour in zebrafish. *Sci. Rep.* **4**, 3810; DOI:10.1038/srep03810 (2014).